C-CORE Publication No. 90-15
pp. 878-889

IAHR
Symposium on Ice 1990
Espoo, Finland
August 20-24, 1990

Proceedings Vol. 2

C-CORE Publication No. 90-15

IAHR Ice Symposium 1990
Espoo

92-01907/

Small Scale Field Indentation Tests on First Year Sea Ice

S.N. Chin — *Institute for Marine Dynamics, National Research Council, St. John's, Newfoundland, Canada

J.P. Nadreau — Ministry for Industry, Science and Technology, Ottawa, Ontario, Canada

B.L. Parsons*

E.V. Guy — Centre for Cold Ocean Resources Engineering, Memorial University of Newfoundland, St.John's, Newfoundland, Canada

ABSTRACT

A series of indentation tests were performed on first year sea ice in Resolute Bay, North West Territories, Canada. Flat and hemispherical indentor heads of varying sizes (28mm to 110mm effective diameter) and different surface roughness (smooth and knurled) were forced horizontally into a prepared vertical ice face. The depth of penetration varied from 1.3 to 5.5 times the diameter of the indentor. The indentor load was measured as a function of the corrected indentation displacement. The ice/structure interaction velocities were limited to a narrow range from 6.05 to 7.32mm/s for the successful tests. In this paper a description of the test apparatus and the procedures are given along with detailed data analysis of successful tests. From these results and recorded video observations the ice failure modes are described for the sea ice indentation processes in the brittle range.

INTRODUCTION

Dynamic ice-structure interactions have been examined through small scale laboratory experiments and theoretical models. A detailed discussion is contained in the review paper by Sodhi (1988). For indentation and penetration of edge loaded freshwater ice sheets over a wide range of aspect ratio (d/h) and interaction rates (>1.0mm/s) Timco (1986) has observed in laboratory experiments five different failure modes ranging from pure crushing to radial/circumferential

cracking and buckling. Similar failure maps were observed in indentation of coastal sea ice by a model test rig, Kawasaki et al (1986). These experimental investigations have shown that there are several factors which affect the load. The indentation factors include the aspect ratio of the interaction, the structure geometry and size, and ice type; the contact factors include the degree of contact area and the ice structure friction coefficient. For low loading rates where creep failure predominates Michel and Touissant (1977) has shown that the indentation pressure is three times the uniaxial compressive strength of the ice. For high loading rates where spalling and crushing occur the problem is not fully understood. The stress state in the penetration of an ice half space is three dimensional and therefore the load levels and failure modes are different than that in an edge loaded ice sheet.

Johnson and Benoit (1987) described a medium scale indentation test program using 1.0 and 3.0m^2 indentors to measure the compressive iceberg strength as a function of impact area. Penetration depths up to 1/5 the indentor diameter were recorded. The indentor velocities were sufficiently high to produce crushing type of failure in the brittle zone.

This paper deals with a preliminary set of field experiments studying the penetration of a small scale indentor head into a vertical ice wall to a maximum depth of 150mm; i.e., up to a maximum of 5 1/2 times the indentor diameter. The results of the tests are presented and penetration and contact factors are discussed in terms of failure modes observed.

TEST APPARATUS

The test apparatus consisted of a hydraulic power unit and a ram actuator unit located in the ice trench. The hydraulic power was supplied by a piston pump with a pressure compensated load sensing device. An 8 horsepower, 4 cycle gasoline engine was used to drive the pump. The line pilot

operated pressure relief valve maintained a line pressure of 13.8MPa. The ram actuator unit as shown in Fig. 1 was a 152.4mm diameter, single acting hydraulic actuator mounted on a rigid base frame with attached skis. Four screw jacks with 120mm steel circular-shaped plates were mounted behind the actuator to distribute the resistance evenly over the trench wall during indentation. A load cell (max. 250kN) was screw mounted on the actuator shaft to measure the indentation load. A fitting was machined at the end of the shaft to permit mounting of different indentor heads. A 200mm stroke rectilinear potentiometer mounted on the jack frame was used to measure the displacement of the indentor head with respect to the frame. Two spring loaded linear potentiometers of 50mm stroke were attached at the opposite ends of the frame with their tips in contact with the ice walls, so that the axial displacements incurred could be measured.

Two indentor head geometries were used: hemispherical and flat. The diameters of the indentor heads were 28, 39, 55, 80 and 110mm, so that the surface area increased by a factor of two with each diameter step. Three surface variations were used with the hemispherical indentor: a) a smooth polished surface; b) knurled surface with spiral groves radiating from the pole; and c) molded, in which the smooth hemispherical head was melted into the ice wall before indentation commenced.

For about 35s of each penetration test the output voltages from the transducers were digitized and stored by a datalogger for later transfer to floppy disk.

TEST PROCEDURE

Initially a 1m deep and .75m wide trench was excavated out of the sea ice using chain saws and picks. The point of indentation was 550 to 750mm down from the top edge of the trench. This was well below the transient zone of the vertical profile and the ice was columnar in structure. The contact surface was smoothed with an ice chisel prior to each test. The actuator unit was then positioned so that the

indentor head was in contact with the ice surface or was molded into the ice. The screw jacks and the two end potentiometers were appropriately adjusted for contact to the respective ice walls.

The tests were carried out at the selected line pressure. For the range of indentor heads used the hydraulic power unit was only able to maintain a narrow range of penetration rate (5.2-7.5mm/s) at a line pressure of 13.8MPa. The datalogger was toggled to sample just prior to release of the relief valve. In addition to video documentation of each indentation test, close up photographs of the damaged sites were taken after the prevalent cracks were marked. Block samples of the damaged ice were taken for crystallographic examination. The tests were conducted at a mean ice temperature of -14°C and pit air temperature ranging from -22 to -10°C.

TEST RESULTS AND DISCUSSION

Field observations and video records indicated key processes which took place in all the penetration tests. The ice at the contact zone was pulverized into fine particles and some of these ice particles were ejected out of the penetration cavity at relatively high speeds. The ejection of the ice particles was not continuous but appeared to coincide with abrupt and finite macroscopic crack growth. Throughout the interaction process there were a large number of microcracks in front of the indentor. Indentor advance was observed to coincide with major macrocracking in the confined damage zone. This implies a three dimensional stress state. Load relaxation coincided with macroscopic crack growth to a free surface when spalling occurred and large pieces of ice broke away from the contact zone. For the range of indentor diameters used in this study cataclastic failure often occurred at the end of the tests, i.e., at penetration depths of greater than 100mm.

A total of 26 tests were performed and seven tests were rejected because the indentor position varied widely during

penetration; abrupt changes in the displacement-time history were recorded in such cases. Since the load and displacement were recorded as a function of time it was necessary to time synchronize the data. All the load displacement plots showed increasing trends and the data was statistically analyzed after removing this trend. A summary of the analyzed maximum and mean loads and determined test parameters is shown in Table 1. The penetration rates (u) shown in Table 1 were determined from the slope of the absolute displacement-time plots, taking into account the frame displacements measured at the two ends of the ice walls. These corrections were not possible in cases where the flaking of the ice wall occurred or in the rejected tests. The apparent strain rates as shown in Table 1 were determined based on the definition given by Ralston (1979), i.e., ($\dot{\epsilon}$=u/2d), assuming it is valid for ice failure in the brittle zone. The variation of the indentor head diameters gave the range of $\dot{\epsilon}$ as $2x10^{-2}$ to $1.4x10^{-1}s^{-1}$.

Typical examples of the ice load-displacement plots of the penetration tests for the smooth hemispherical and flat indentor heads of diameters 55mm and 80mm, respectively, are shown in Figures 2 and 3. These two plots show different forms of irregular saw-shaped cyclic fluctuations. The increasing trend in the plots is a consequence of the confinement stress state which develops as the indentor head advances. The shape of the indentor heads appears to affect the load-displacement history during penetration of ice. For the hemispherical indentor there is a sharply defined load buildup before subsequent relaxation. A wave like fluctuation is observed in the load-displacement plot of the flat head indentor. The amplitude of the load fluctuation (i.e., peak-valley magnitude) plotted against displacement for the smooth hemispherical and flat indentors of Figures 2 and 3 are shown in Figures 4 and 5, respectively. In Figure 4, there is greater variation in the load magnitude than in Figure 5. The stress distribution about the surface of the hemispherical head is continuous with the maximum value at the pole. The stress gradient along the curvature permits stress relief and facilitates the ejection of ice particles.

For the flat indentor, a stress singularity occurs along the edge where cracks initiate readily but this only relieves the load partially; and thus does not permit the complete removal of damaged ice.

Sanderson (1988) showed that for a number of small scale measurements on S-2 sheet ice and at indentation rates (u/d) of less than 10^{-2} s^{-1}, the average peak stress (σ_p) which depends on strain rate is of the form:

$$\sigma_p \propto (u/d)^{1/n} \qquad (1)$$

where n is in the range 3-4, and the peak measured stress was approximately 20MPa. In contrast to the latter, the present stresses are generated in a triaxial stress field, and at strain rates greater than 10^{-2} s^{-1}. Using the projected area of the indentor head the maximum average pressure for the penetration tests can be estimated. The plot of maximum average pressure against strain rate is shown in Figure 6. There is some scatter in the plot but for the hemispherical indentor heads the data points show a similar exponential trend. Even in the knurled condition the effect of friction was negligible. For the relation in Eq. 1. the exponent n ranged from 1.33 to 1.84. over one order of magnitude variation in strain rate. The stress state in front of the forced indentor gave maximum average pressures of much greater than 20MPa with the maximum value of 110MPa when the 110mm flat indentor head was used. Instantaneous local pressures are much higher than those estimated because the contact area at any given time during the penetration process is much smaller than the projected area.

SUMMARY AND CONCLUSIONS

The series of field tests was concerned with the penetration of two different types of indentor head into a semi-infinite vertical ice wall. The tests were conducted at high loading rates and brittle ice failure predominates.

The penetration tests gave maximum average pressures in the range of 20-110MPa which are much higher than observed in

small scale laboratory indentation test on an ice sheet at similar strain rates. The load showed an increasing trend with penetration depth. The effect of the three dimensional stress distribution in the ice in front of the penetrating indentor is seen in the increase and fluctuation of the load with depth, and in the high maximum average pressure measured. This study indicated that the type of load displacement history is dependent on indentor geometry and strain rates. The inhomogeneity of the sea ice structure may also have a significant effect on the load levels recorded. The vigorous ejection of the ice particles during indentor penetration follows macrocracking which suggests a conversion to surface energy of damaged ice and to kinetic energy.

The data acquisition system used in this experiment did not provide a sufficient high data sampling rate necessary to capture all the instantaneous maximum and minimum loads in the penetration process. Lateral and vertical variations in the position of the indentor during penetration invalidated a number of tests.

ACKNOWLEDGEMENTS

This project was a cooperative effort between IMD/NRC and C-CORE of Memorial University St.John's. Newfoundland. The authors wish to express their appreciation to Dr. F.M. Williams and Mr. C. Pierce III, and all those involved in the field work.

REFERENCES

Johnson, R.C., and, J.R. Benoit, 1987. Iceberg impact strength. Offshore Technology Conference. Houston, USA. Vol. 4. pp. 417-423.

Kawasaki, T., et al., 1986. Indentation tests of laboratory and field ice sheets. Polartech '86 Helsinki, Finland. Vol. 2. pp. 712-724.

Michel, B. and, N. Touissant, 1977. Mechanisms and theory of indentation of ice plates. Journal of Glaciology, Vol. 19 No. 81, pp. 285-300.

Ralston, T.D., 1979. Sea ice loads. Technical Seminar on

Alaska Beaufort Sea Gravel Island Design, Exxon Company. U.S.A

Sanderson, T.J.O., 1988. Ice Mechanics :Risks to Offshore Structures. Graham & Trotman. Great Britain.

Sodhi, D.S., 1988. Ice-induced vibrations of structures. Proceedings, IAHR International Symposium of Ice, Sapparo, Japan, Vol. 2, pp. 625-657.

Timco, G.W., 1986. Indentation and penetration of edge-loaded freshwater ice sheets in the brittle range. Proceedings, OMAE Symposium. Tokyo, Japan. Vol. 4, pp 445-452.

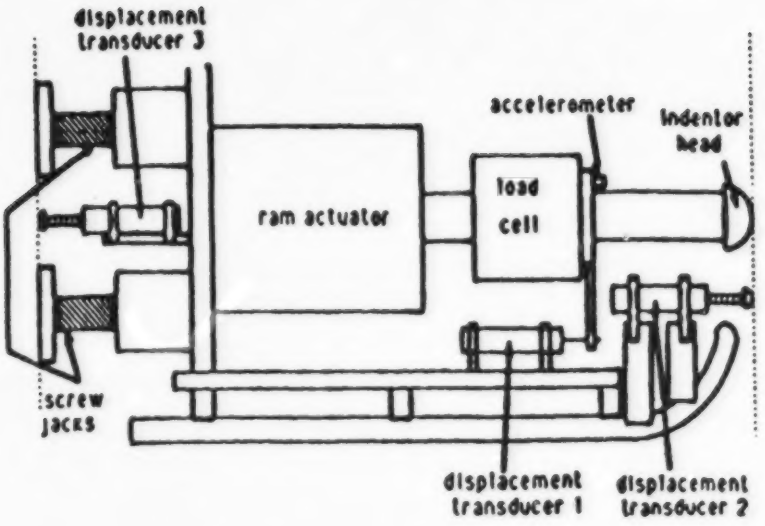

FIGURE 1 : Side view of ram actuator unit

TABLE 1: Summary of Ice Loads and Parameters for Range of Penetration Tests

INDENTOR		ICE LOAD				Penetration rate (mm/s)	Penetration depth (mm)	Apparent strain rate (1/s)
Type	Diameter (mm)	Maximum (kN)	Mean (kN)	Slope (kN/mm)	Off set (kN)			
smooth (h)	28.0	40.870	12.833	0.104	8.873	7.081	114.783	0.126
	38.0	76.281	18.822	0.208	5.388	7.324	129.801	0.094
	55.0	102.355	28.217	0.233	10.957	7.230	146.689	0.066
	80.0	178.598	51.102	0.610	11.917	6.659	135.581	0.041
	110.0	210.107	69.039	0.628	29.184	6.448	139.063	0.029
knurl (h)	28.0	41.055	10.500	0.200	4.844	6.984	136.100	0.124
	38.0	65.385	21.988	0.239	5.463	7.488	136.936	0.096
	80.0	78.675	30.804	0.289	21.079	8.325	155.220	0.039
	80.0	160.353	44.437	0.431	11.486	7.837	152.378	0.044
molded (h)	28.0	36.254	13.107	0.058	8.784	7.387	152.868	0.134
	38.0	62.998	15.933	0.187	8.711	7.433	89.756	0.098
	55.0	131.488	34.214	0.253	17.891	8.781	132.070	0.082
	80.0	143.495	36.211	0.152	26.411	6.599	118.215	0.041
	80.0	193.731	54.072	0.179	44.438	7.263	109.628	0.045
flat	28.0	69.300	16.356	0.123	8.387	7.216	131.883	0.129
	38.0	83.847	16.507	0.144	10.713	8.048	77.208	0.079
	64.0	180.080	51.032	0.183	38.709	7.671	147.129	0.055
	80.0	229.889	94.553	0.612	49.535	8.687	143.190	0.043
	80.0	203.013	88.771	0.738	36.382	8.749	133.703	0.042

h: hemispherical indentor head

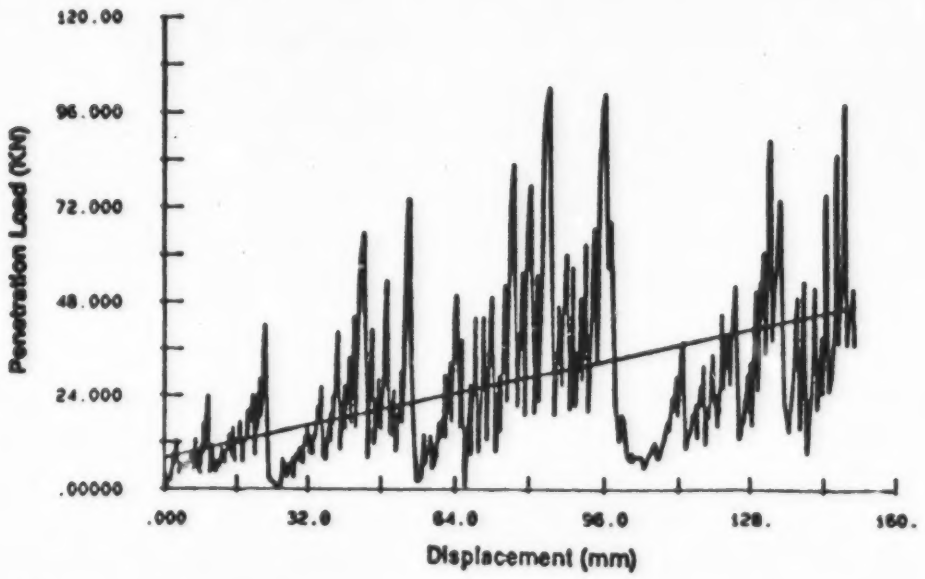

FIGURE 2 : Typical Load-Displacement curve for smooth hemispherical Indentor

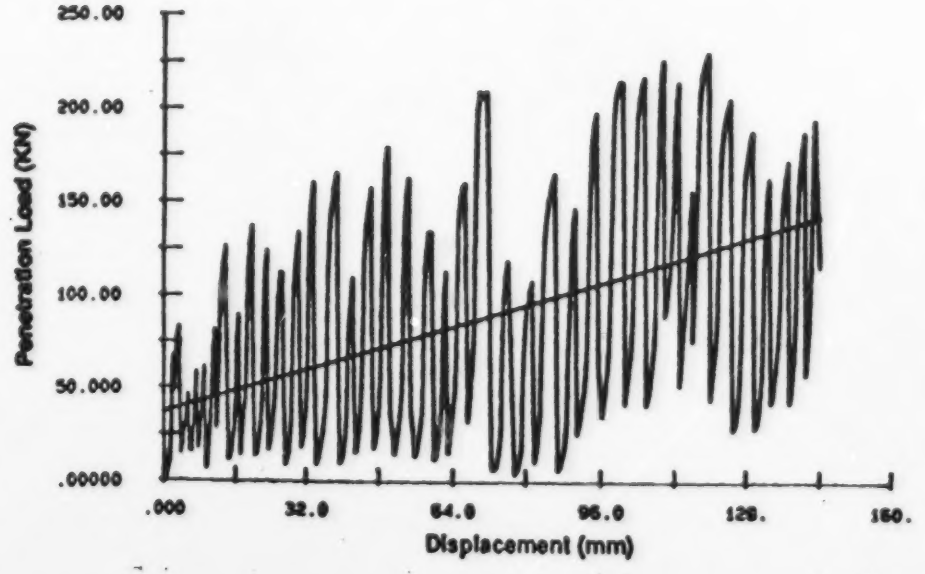

FIGURE 3 : Typical Load-Displacement curve for flat Indentor Head

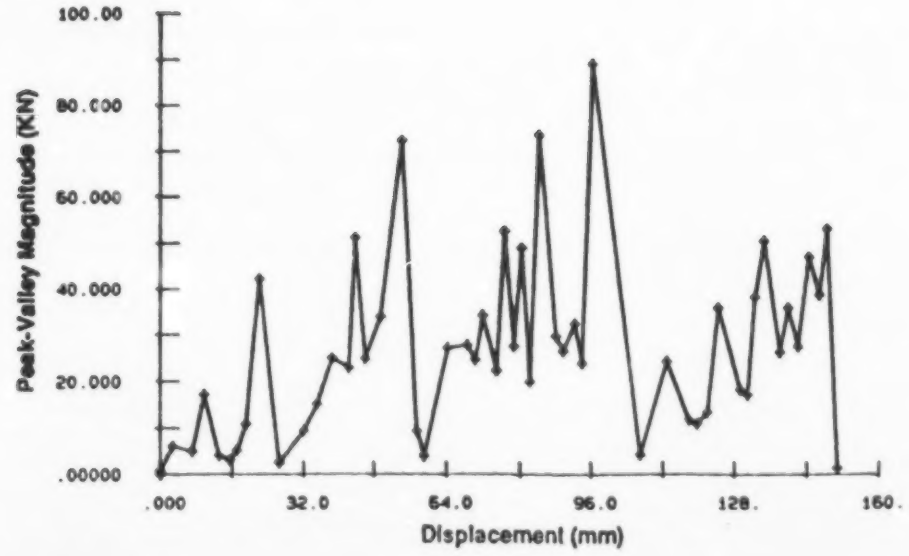

FIGURE 4 : Typical plot of Peak-Valley Magnitude against Displacement for smooth hemispherical Indentor Head

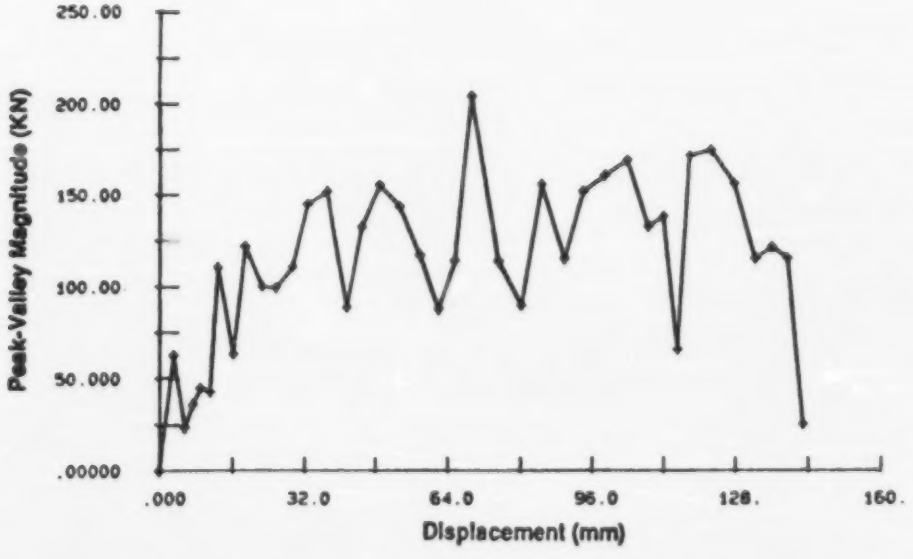

FIGURE 5 : Typical plot of Peak-Valley Magnitude against Displacement for flat Indentor Head

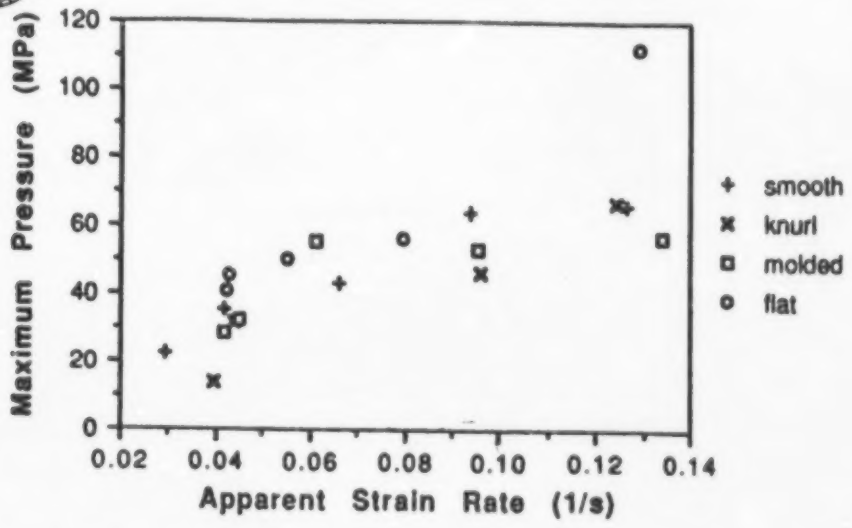

FIGURE 6 : Maximum Pressure against Apparent Strain Rate